International Journal of ChemTech Research
CODEN (USA): IJCRGG, ISSN: 0974-4290, ISSN(Online):2455-9555
Vol.10 No.15, pp 146-162, 2017

Spectro-thermal characterization and molecular modeling of bioactive metal complexes of 4 -diethylaminosalicyldeoxime

Bibhesh K Singh[1]*, Jagdish Chandra[1], Hament K. Rajor[2], Pinkee[1]

[1]Department of Chemistry, Govt. Postgraduate College, Ranikhet, Uttarakhand-263645, India
[2]Department of Chemistry, Ramjas College, University of Delhi, Delhi-110007, India

Abstract : Newly synthesized ligand 4-diethylaminosalicyldeoxime (4-DEASDOX) and their Co(II), Ni(ii), Cu (II), and Zn(II) complexes have been prepared and characterized by different physicochemical techniques. The ligand 4-diethylaminosalicyldeoxime behaves as a bidentate ligand forming neutral metal chelates through the phenolic oxygen and the oxime nitrogen. The M-O stretching frequencies for the transition metals show good agreement with the Irving-William's stability order. Similar trend is seen for the M-N stretching frequencies in vibrational spectra and the shift in transitions from electronic spectral data for the metal complexes. Mass spectrum explains the successive degradation of the molecular species in solution and justifies ML_2 complexes. Electronic spectra and magnetic susceptibility measurements suggest square planer geometry of the metal complexes. Thermodynamic activation parameters were computed from the thermal data using Coats and Redfern method, which confirm first order kinetics. The geometry of the complexes has been optimized with the help of molecular modeling. The bio-efficacy of free ligand and its metal complexes have been examined against the growth of bacteria and pathogenic fungi *in vitro* to evaluate their anti-microbial potential.

Keywords : Bioactivity, Metal complexes, Molecular modeling, Salicyldeoxime, Spectra, Thermal studies.

1. Introduction

There is currently a renewed interest in the coordination chemistry of structurally modified bio-ligands. Oximes play an important role in the development of transition metal coordination chemistry due to their versatile bonding mode. Oximes and their derivative are important intermediates in organic synthesis[1]. Many drugs have an oxime group in their structure, which is then frequently used for molecular modifications to develop new drugs and for synthesis of many functional groups as a starting point [1]. Oximes have both Nitrogen and Oxygen donor atoms; therefore, they link metals forming chelate complexes. On the other hand, some of the oximes and their metal complexes exhibit liquid crystalline properties and having photo or electro-driven emitting properties[2].

Anti-tumour copper salicylaldoxime complex which induces Topoisomerase I (topo II) to form single-strand nicks in DNA and poisons its activity, which could be one of the possible mechanisms for the anti-cancer activity of this complex. Copper salicylaldoxime complex inhibits the enzyme activity through induction of enzyme linked single-strand breaks in the DNA and may inhibit topo II dimerization, which may lead to the formation of single-strand breaks[3]. Topoisomerase II is a nuclear enzyme which is crucial for resolving DNA knots in the chromosomes during replication, transcription and cell division during chromosome segregation[3].

In acid medium, salicylaldoxime functions as a molecular ligand (H_2Sal), which brings about a decrease in electron density on donor atoms when compared with the HSal anion. Thus the ability of the used ligand to stabilize the central atom in unusually high oxidation states is impaired. The reaction of $Ni(HSal)_2$ with bromine involves a preferential attack on the aromatic ring of ligand. The possibility of oxidizing with peroxodisulfate is negatively affected by separation of nickel(II) salicylaldoximate from the water- organic solvent (ethanol, acetone) mixture[4]. However, with increasing use of oxime as drugs and pesticides, the intake on these chemical followed by enzymatic oxidation may result in the formation of a variety of reactive intermediates, which may lead to cell and tissue damage [5].

Spectral and thermal characterization serves as important tools for the interpretation of the structures of bio-molecules. Therefore, we report here in the synthesis and characterization of the complexes of 4-diethylaminosalicyldeoxime (DEASDOX) bidentate ligand with transition metal (II) ions. The geometry of the complexes has been optimized by molecular modeling studies. The bioactivity of the ligand and its metal complexes possess antimicrobial properties.

2. Experimental

All the chemicals used were of analytical grade and used as procured. Solvents used were of analytical grade and were purified by standard procedures. The stoichiometric analyses (C, H and N) of the complexes were performed using Elementar vario EL III (Germany) model. Metal contents were estimated on an AA-640-13 Shimadzu flame atomic absorption spectrophotometer in solution prepared by decomposing the respective complex in hot concentrated HNO_3. Their IR spectra were recorded on Perkin–Elmer FT- IR spectrophotometer in KBr and polyethylene pellets in the range 4000-400 cm^{-1} and 400-100 cm^{-1}, respectively.^{1}H-NMR spectra were recorded in DMSO-d_6 solvent on a Bruker Advance 400 instrument. Proton chemical shifts are reported in parts per million(ppm) relative to an internal standard of Me_4Si.The UV-Visible spectra were recorded in DMSO on Beckman DU-64 spectrophotometer with quartz cells of 1 cm path length from 200-900nm and mass spectra (TOF-MS) were recorded on Waters (USA) KC-455 model with ES^+ mode in DMSO. Magnetic susceptibility measurements were carried out at room temperature in powder form on a vibrating sample magnetometer PAR 155 with 5000G-field strength, using $Co[Hg(SCN)_4]$ as the calibrant (magnetic susceptibility $\approx$ 1.644 $\times 10^{-5} cm^3 g^{-1}$). Rigaku model 8150 thermoanalyser (Thermaflex) was used for simultaneous recording of TG-DTA curves at a heating rate of $10^o min^{-1}$. For TG, the instrument was calibrated using calcium oxalate while for DTA, calibration was done using indium metal, both of which were supplied along with the instrument. A flat bed type aluminium crucible was used with α-alumina (99% pure) as the reference material for DTA. The number of decomposition steps was identified using TG. Molecular modeling of the proposed structure of the complexes was performed using HyperChem professional version 7.51 program package[6]. *In vitro* antibacterial activity of the synthesized compounds against *Streptococcus, Staph, Staphylococcus aureus* and *Escherchia coli* bacteria were carried out using Muller Hinton Agar media(Hi media) . The activity was carried out using paper disc method[7]. Base plates were prepared by pouring 10ml of autoclaved Muller Hinton agar into sterilized Petri dishes (9 mm diameter) are allowing them to settle. Molten autoclaved Muller Hinton had been kept at 48°C was incubated with a broth culture of the *Streptococcus, Staph, Staphylococcus aureus* and *Escherchia coli* bacteria and then poured over the base plate. The discs were air dried and placed on the top of agar layer. The plates were incubated for 30 h and the inhibition zones (mm) were measured around each disc. The Antifungal activity of the complex was checked by dry weight method for the *Alternarie alternate, Aspergillus flavus, Aspergillus nidulans* and *Aspergillus niger* fungi. The complexes were directly added to the growth medium in varying concentration. The actively growing mycelia (of the test fungi) were placed on the medium with the help of inoculums needle and incubated at 27±2 ^{0}C for 7 days. The medium with the test solution served as treated while without them as control or check. The resulting mycelia mats in each set were carefully removed, washed, dried and then weighed separately. The fungal growth was calculated from the following relation:

$$\text{Fungal growth inhibition (\%)} = \frac{Cg - Tg}{Cg} \times 100$$

where *C*g is the average growth in the 'control' or 'check' set

*T*g is the average growth in the treated set.

2.1. Synthesis of ligand and complexes

2.1.1. Synthesis of ligand

The ligand(Fig.1) has been synthesized by mixing 4-diethylaminosalicyldehyde (0.01M) with hydroxylamine hydrochloride(0.01M) in ethanol(25ml) at room temperature and also added triethylamine drop wise with constant stirring by keeping the pH 8-9 for 48*h*. The white precipitate was filtered, washed with ethanol and dried under vacuum over silica gel.

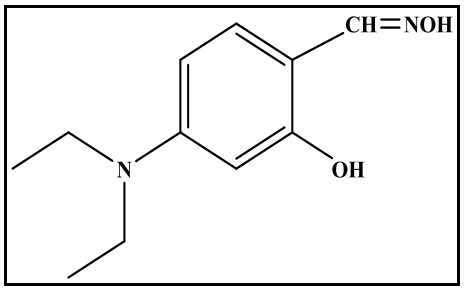

Fig.1 Structure of the ligand: 4-diethylaminosalicyldeoxime(4-DEASDOX)

2.1.2 Synthesis of complexes

To 50 ml 0.2M aqueous solution of the salts of respective metal chlorides, 50ml. of 0.4M solution of the ligand 4-diethylaminosalicyldehydeoxime in 50% ethanol was added. The precipitated complexes were digested, filtered, washed first with hot water and then with 20% ethanol and finally dried at 110–120 ^{0}C in an air oven. The Co(II) complex formed brown, Ni(II) complex formed Light green, Cu(II) complex formed Light blue and Zn(II) complex formed white precipitate. The solubility of these complexes is sparingly soluble in water and completely soluble in DMSO, Acetone etc.

3. Results and discussion

On the basis of elemental analysis data(Table1), the complexes have the general composition ML_2, where M = Co(II),Ni(II),Cu(II) and Zn(II); Ligand = 4-diethylaminosalicyldeoxime.The complexes were obtained in powder form. These were found to be sufficiently soluble in Acetone and DMSO for spectral measurements. Various attempts to obtain the single crystals of the complexes have so far been unsuccessful. However, the analytical and spectroscopic data enables us to predict possible structures. The molecular modeling helps to determine the bond angles, bond length and supports the possible geometry of the complexes.

3.1 Spectroscopic and magnetic characterizations

The ^{1}H NMR spectra of a DMSO-d_6 solution of the oxime ligand(DEASDOX) show well resolved signals as expected(Figure 2: ^{1}H NMR of the ligand). The spectrum of the oxime ligand shows a doublet at 1.2ppm, (6H), doublet at 3.39ppm(4H), singlet peak at 6.2ppm, 7.3ppm and 8.18ppm of benzylidenimin group, and singlet at 2.0ppm(alcoholic H) and 5.0 ppm(aromatic C-OH).The ^{1}H -NMR spectra of complex II and complex IV show the resonance with expected integrated intensities. In both the complexes, no signal of the phenolic hydrogen indicates deprotonation of the ortho-hydroxyl group on complexation. Furthermore, the aliphatic protons are not greatly affected upon complexation.

Table 1: Analytical and physical data of ligand and their metal complexes

S No	Compound/complex (Empirical formula)	Color	Decomposition temperature (°C)	Yield (%)	Analysis found (Calculated(%) C H N M	μ_{eff}(BM)	Electronic spectra(nm)
1	Ligand ($C_{11}H_{16}O_2N$)	White	159	85	63.8 (63.78) 7.30 (7,32) 13.50 (13.48) -	-	285,370
2	Complex I [Co($C_{11}H_{14}O_2N_2$)$_2$]	Light Brown	246	80	28.03 (28.22) 2.97 (2.99) 5.94 (5.99) 12.50 (12.61)	2.34	290,372,422,530
3	Complex II [Ni($C_{11}H_{14}O_2N_2$)$_2$]	Light green	298	86	28.04 (28.23) 2.97 (2.98) 5.94 (5.98) 12.45 (12.51)	diamagnetic	283,375,655,557
4	Complex III [Cu($C_{11}H_{14}O_2N_2$)$_2$]	Light blue	287	82	27.76 (27.81) 2.94 (2.98) 5.88 (5.90) 13.35 (13.57)	1.74	280,369,515,650
5	Complex IV [Zn($C_{11}H_{14}O_2N_2$)$_2$]	white	315	80	27.65 (27.77) 2.93 (2.99) 5.86 (5.91) 13.78 (13.88)	diamagnetic	282,378

Table 2. IR spectral data (cm^{-1}) of ligand and its metal complexes

Frequency	Ligand	Complex I	Complex II	Complex III	Complex IV
ν $(OH)_{NOH}$	3280(s)	2988(w)	2994(w)	2996(w)	2971 (w)
ν (C=N)	1660(s)	1640(s)	1647(s)	1645(s)	1643(s)
δ (NOH)	1458	1452(s)	1455 (w)	1450(s)	1453(s)
ν (CH)	2852(s)	3022 (s)	2989(s)	2922(s)	3023(s)
ν (N-O)	860	868	890	872	878
δ (O-M-O)	-	185	188	192	179
ν (M-O)	-	326(m)	321(m)	388(m)	332(m)
ν (M-N)	-	287(m)	279(m)	276(m)	293(m)
ν (CH_3)	1376	1348	1351	1349	1358
ν (C-O)	1205	1195	1187	1192	1188
δ (O-M-N)		231	235	215	239

s = strong;m = medium, w = weak

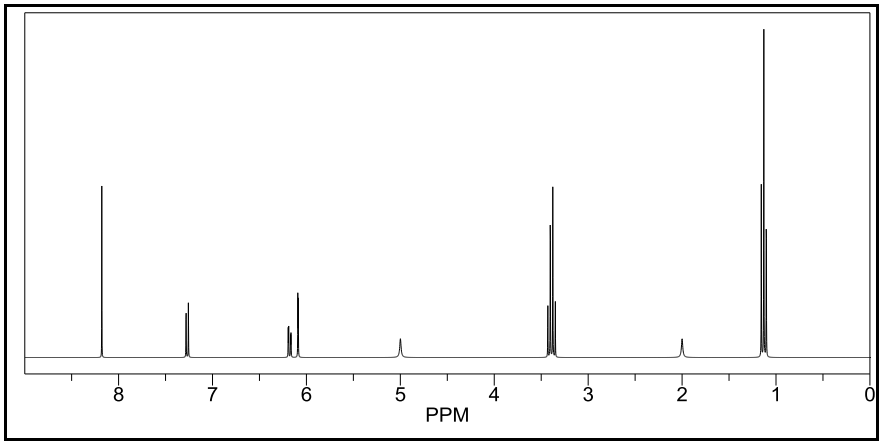

Fig.2 ^{1}H- NMR- Spectra of the ligand

The vibrational spectrum of the free ligand showed a broad band between 3100- 3500 cm^{-1}, which can be attributed to phenolic OH group. This band disappears in all complexes, which can be attributed to the involvement of phenolic OH in coordination. The involvement of deprotonated phenolic moiety in complexes is confirmed by the shift of ν(C-O) stretching band observed at1205 cm^{-1} in the free ligand to a lower frequency to the extent of 10–20 cm^{-1}[8]. The shift of ν(C-O) band at 1205 cm^{-1} to a lower frequency suggests the weakening of ν(C- O) and formation of stronger M - O bond. The broad and low intensity bands due to ν(O-H) modes of N- OH groups in the 3300–3000 cm^{-1} frequency range shifted to the lower frequency region (2900–3000 cm^{-1}) which suggests the weakening of N-OH bond and formation of M- N bond[9] . The medium bands observed in the 1650–1610 cm^{-1} frequency ranges in complexes were assigned to ν(C= N) mode (figure 3a-e: IR spectrum of the ligand and complexes). The shift of ν(C= N) vibration in all the complexes to a lower frequency suggests that the nitrogen atom of the ring contributes to the complexation. The lower ν(C= N) frequency also indicates stronger M -N bonding[10,11]. The IR spectrum of the ligand showed the ν(N-O) band appears at 860 cm^{-1}(Table 2: IR sprecral data of ligand and complexes). So, on M-N interaction, ν(N-O) appeared at higher frequencies, indicating that N-O bond length decreases. The positive ν(N-O) shift indicates strengthening of the M- N bond. In the IR spectra of the complexes, a band is observed between 285 and 295 cm^{-1} that is attributed to the ν(M- N) stretching vibrations. Another band appeared between 640 and 655 cm^{-1}, which is assigned to the interaction of phenolic oxygen to the metal atom, i.e.,the stretching vibrations ν(M-O)[8].

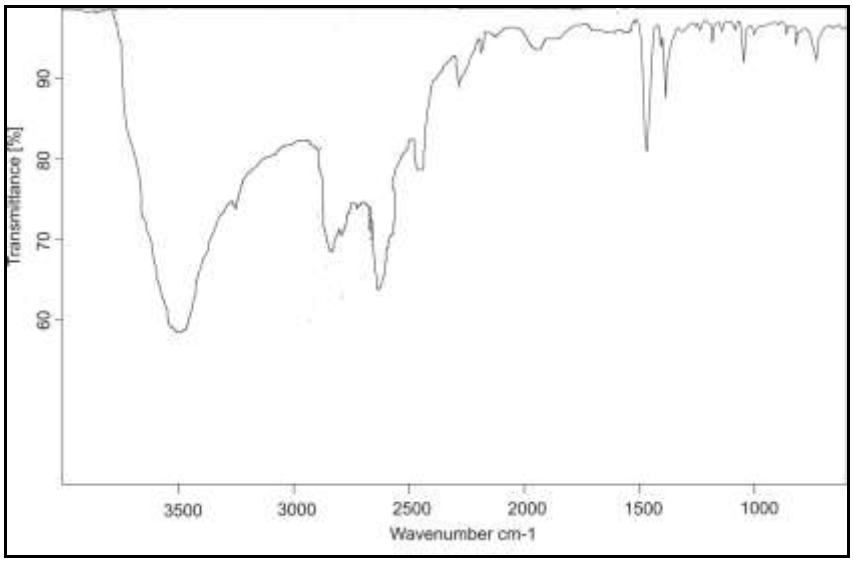

Fig.3a: IR spectrum of the ligand

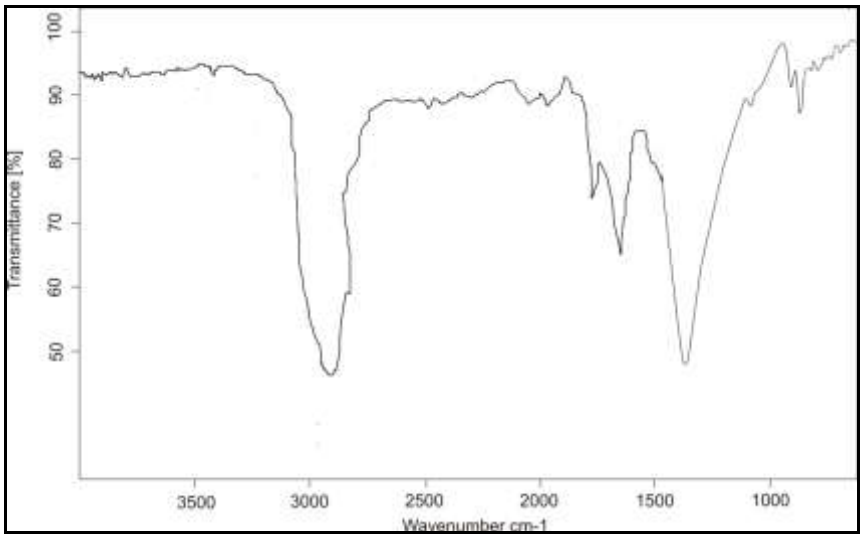

Fig.3b: IR Spectra of the complex I

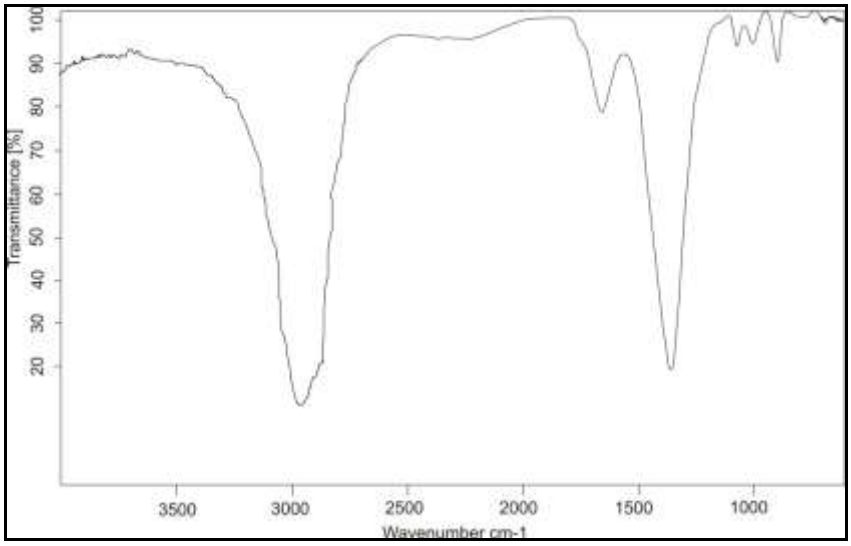

Fig.3c IR Spectra of the complex II

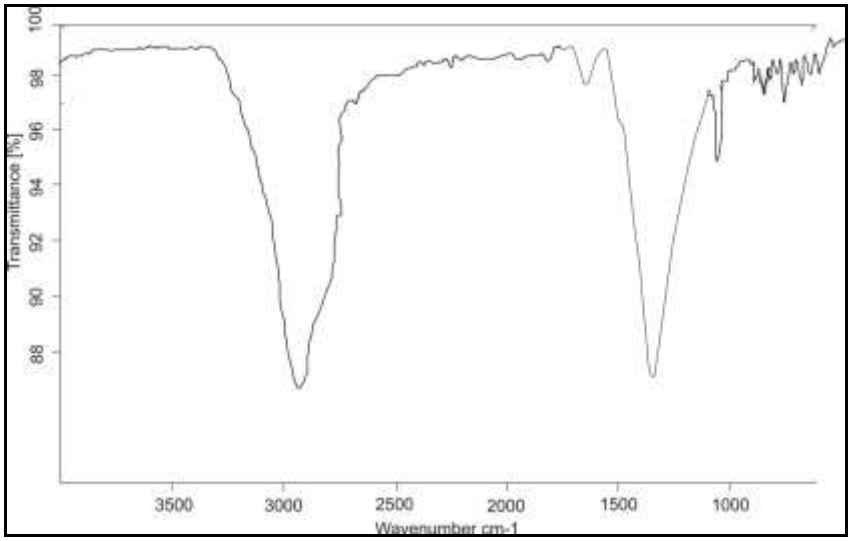

Fig.3d: IR Spectra of the complex III

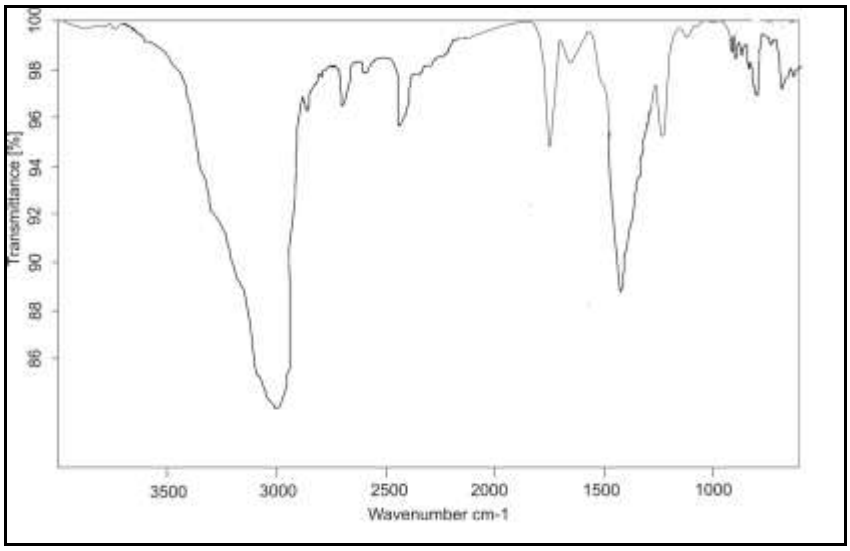

Fig.3e: IR Spectra of the complex IV

The electronic spectra of the complexes were recorded in DMSO. The bands in the 200-380 nm regions coincide with the bands observed in the free ligand. Two relatively less intense bands (n →π* and π → π*) occur in the 200-380 nm region, these can be assigned to phenolic oxygen to metal and C=N to the metal charge transfer transitions, respectively. The electronic spectral data the Co(II) complexes show absorption bands at 530 nm and 422 nm assignable to $^2B_{2g}\rightarrow{}^4E_g(P)$ and $^2B_{1g}\rightarrow{}^4A_{2g}$ (P) transitions, respectively, suggest square planar geometry of the complexes [12,13], which is also corroborated by magnetic moment value given in Table 1. The reason for the departure from the spin only value lies partly in the existence of the second order Zeeman effect between the ground and the higher ligand field terms [14]. However, it lies mainly in the fact, that in the presence of spin-orbit coupling, the quenching effect of the ligand field cannot be complete. Spectra of the nickel(II) complex shows an absorption band at 655nm, assignable to a $^1A_{1g}\rightarrow{}^1A_{2g}$ transition and a shoulder in the region 550–560 nm corresponding to a $^1A_{1g}\rightarrow{}^1B_{1g}$ transition which are consistent with square planar stereochemistry about the nickel(II) ion. It can be explained with the planar ligand set causes one of the d-orbitals ($dx^2–y^2$) to be uniquely high in energy and the eight electrons can occupy the other four d-orbitals but leave this strongly antibonding one vacant. The diamagnetic nature of the Ni(II) complexes further supports its square planar nature. The electronic spectrum of the Cu(II) complex shows very intense absorption bands in the UV region, attributed to ligand transitions(n →π* and π → π*), and a characteristic broad bands in visible region at 650 nm and 515 nm assignable to $^2B_{1g}\rightarrow{}^2E_g$ and $^2B_{1g}\rightarrow{}^2A_{1g}$ transitions respectively, indicates the possibility of square planar geometry of metal complex. The Cu(II) complex has magnetic moment value 1.74 BM reveals square planar geometry around the metal ion[12]. Zn(II) complex is diamagnetic in nature and their electronic absorption spectrum does not have d-d transition bands. These complexes assigned square planer geometry.

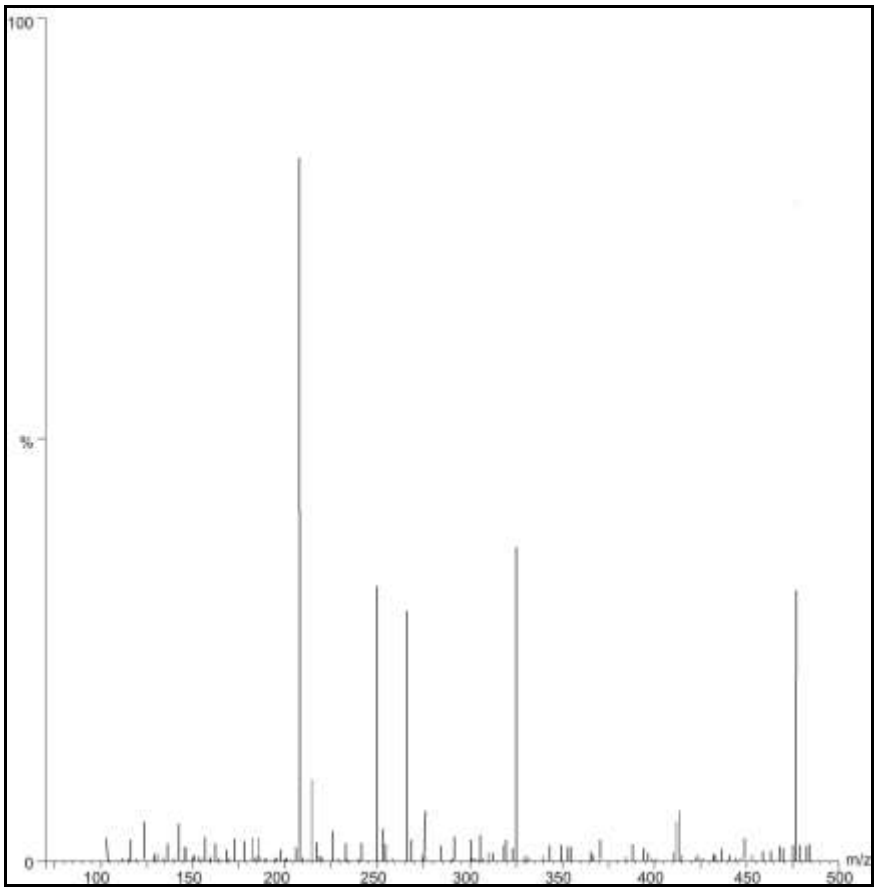

Fig.4 a: TOF- mass spectrum of the complex I

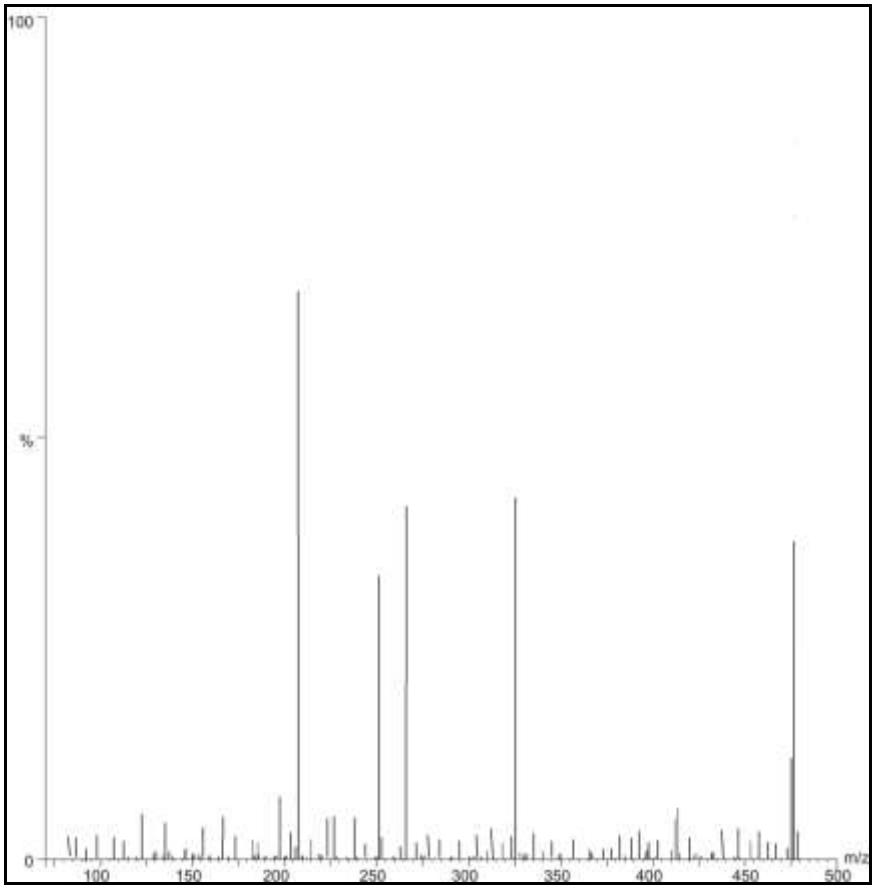

Fig.4b: TOF- mass spectrum of the complex II

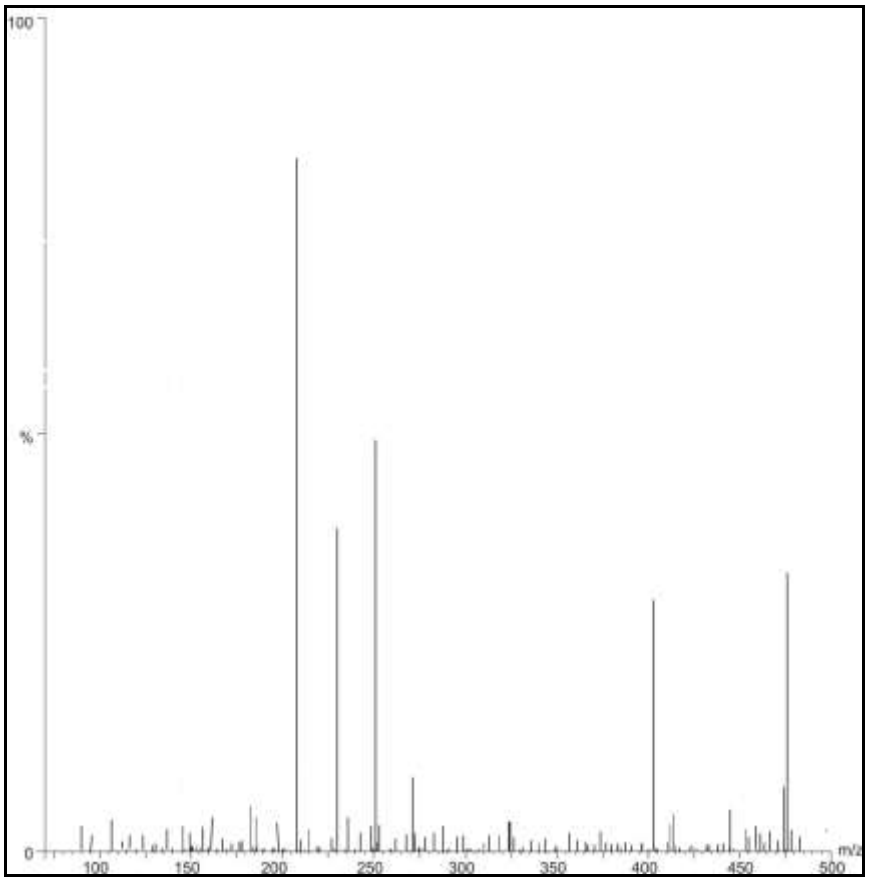

Fig.4c: TOF- mass spectrum of the complex III

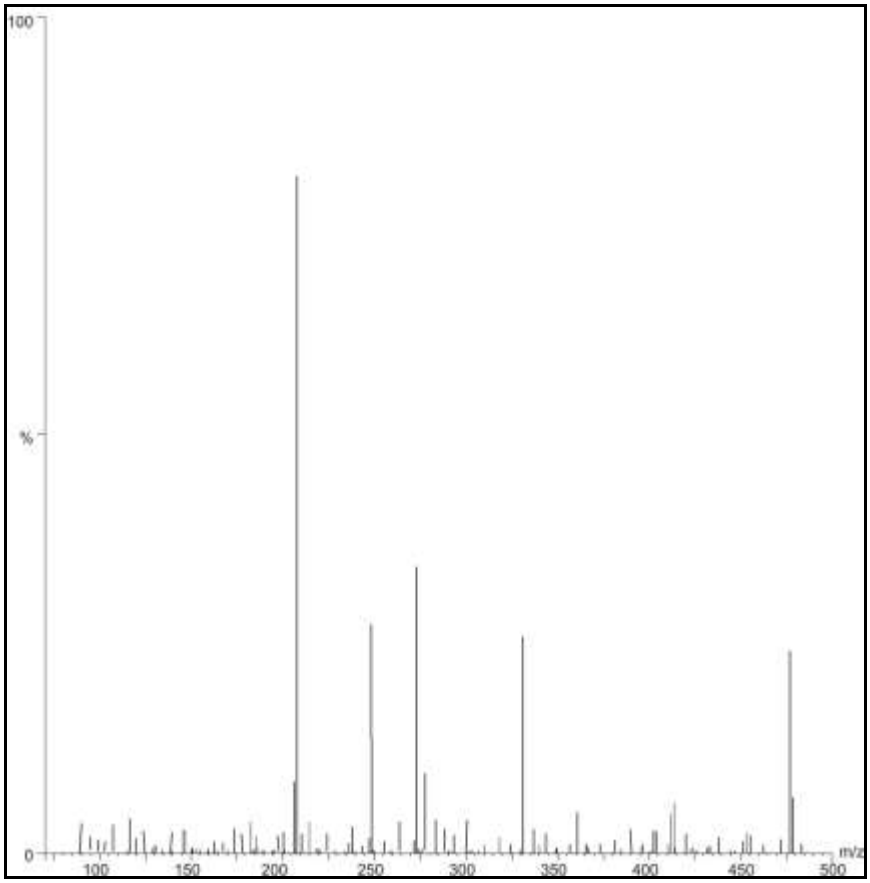

Fig.4d: TOF- mass spectrum of the complex IV

Mass spectrometry has been successfully used to investigate molecular species in solution [15]. The pattern of the mass spectrum gives an impression of the successive degradation of the target compound with the series of peaks corresponding to the various fragments. The intensity gives an idea of stability of fragments. The mass spectrum of the ligand having a molecular ion peak at 208{85% m/z} confirms purity of the ligand. The recorded molecular ion peaks of the metal complexes have been used to confirm the proposed formula. All the synthesized complexes containing metal ion were confirmed by good agreement between the observed and calculated molecular formula (Figure 4a-d: TOF-Mass spectrum of the complexes). Elemental analysis values are in close agreement with the values calculated from molecular formulas assigned to these complexes, which further supported by the TOF-mass studies. In the TOF–mass spectra of metal complexes initial fragmentation pattern is similar, a binuclear nature for these complexes $[M(L_2)]^+$ can be deduced. The mass spectrum of the complexes having a molecular ion peak at 471/472{39% m/z in complex I}, 470/471{40% m/z in complex II}, 476/477{30% m/z in complex III) and 476/477{25% in complex IV} respectively, further confirming the purity of the complexes. The prominent peak in the middle of the degradation pathway appears in nearly all the complexes at positions (m/z values) 325-332(nearly 28% m/z), and 248-252(nearly 39% m/z) are degradation of $[C_8H_{22}N_2]^+$ molecule which are results of demetallation and subsequently a partial intramolecular hydrogen bonding. Likewise peaks around 266-274(m/z) and 208(m/z) are attributable to unstable monomeric species as $[M(L)]^+$ and $[H_2L]^+$ respectively, usually present in the mass spectra of these systems [16].

Table 3: Thermodynamic activation parameter of metal complexes

Complexes	Order(n)	Steps	E*(Jmol^{-1})	A($\times10^5$s^{-1})	ΔS*(JK^{-1}mol^{-1})	ΔH*(J mol^{-1})	ΔG*(k J mol^{-1})
Complex I	1	I	44.11	0.56	-213.44	17.95	84.96
		II	45.39	0.43	-218.35	118.62	120.21
Complex II	1	I	20.66	0.16	-243.05	65.26	102.39
		II	31.53	0.29	-241.00	223.75	137.11
Complex III	1	I	19.11	0.35	-258.94	78.71	116.25
		II	21.84	0.34	-259.56	181.56	161.89
Complex IV	1	I	20.91	0.15	-244.85	112.33	116.42
		II	22.05	0.12	-248.75	442.57	157.90

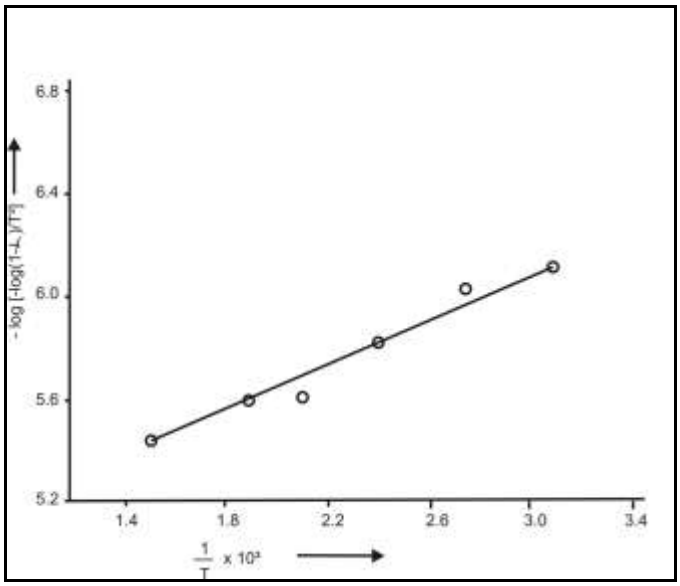

Fig. 5a: Linearization plot of Complex I

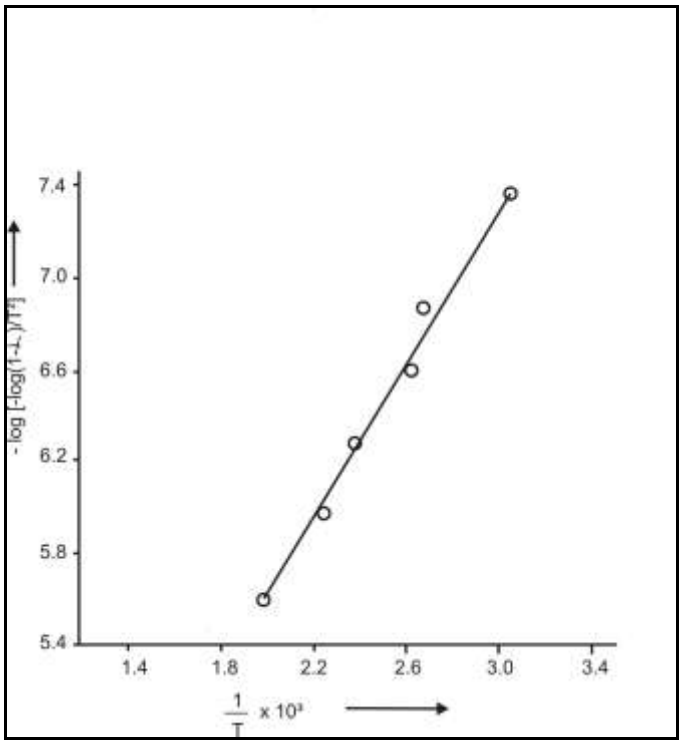

Fig. 5b: Linearization plot of Complex II

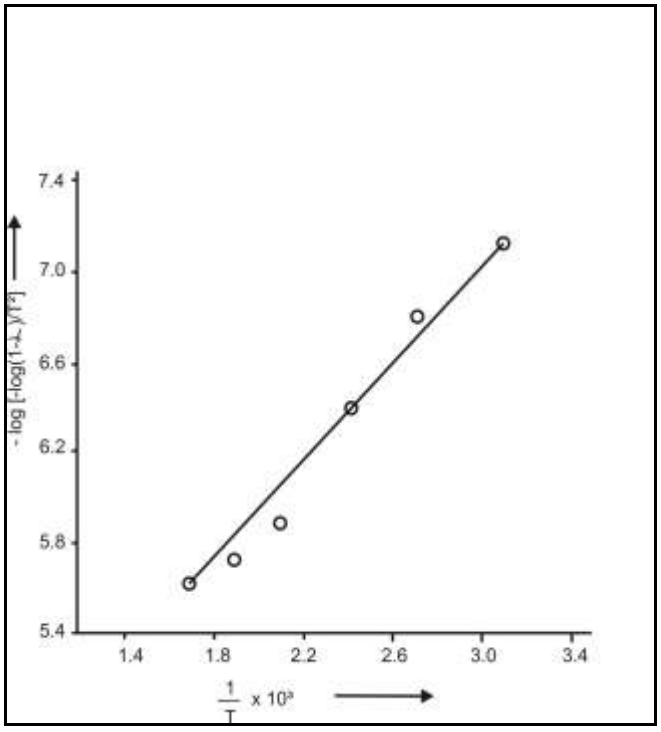

Fig 5c: Linearization plot of Complex III

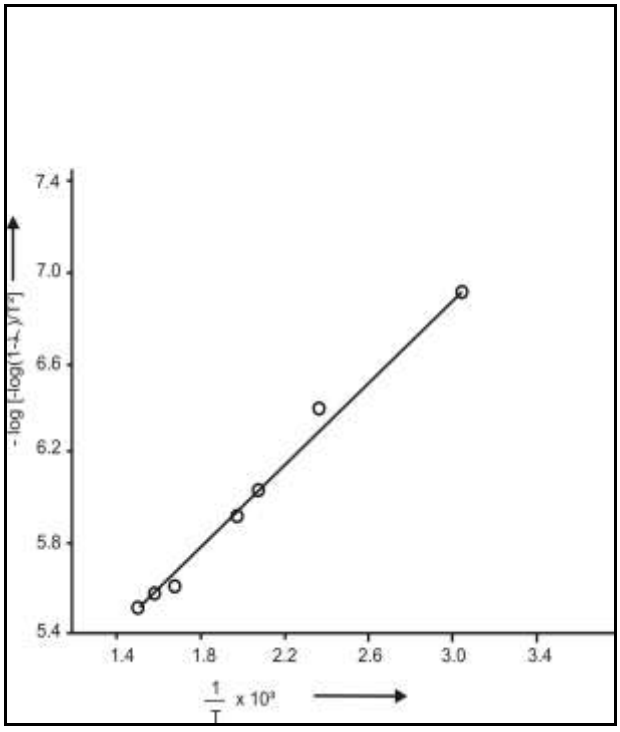

Fig 5 d: Linearization plot of Complex IV

3.2. Kinetics of thermal decomposition

Thermogravimetric (TG) and differential thermogravimetric analyses (DTA) were carried out for metal complexes in ambient conditions. The correlations between the different decomposition steps of the complexes with the corresponding weight losses are discussed in term of the proposed formula of the complexes. In the complexes, loss of (C_4H_8+ NH_3) molecules takes place in the temperature range 380 – 450K followed by the decomposition of the organic moiety with the formation of metal oxide as residue in the temperature range 500-680K[17]. This has been again confirmed by comparing the observed/estimated and the calculated mass of the pyrolysis product. On the basis of thermal decomposition, the thermodynamic activation parameters(Table 3) such as activation energy (E*), enthalpy of activation (ΔH*), entropy of activation (ΔS*), free energy change of decomposition (ΔG*) were evaluated by employing the Coats – Redfern relation [18]. The Coats and Redfern linearization plots (figure 5a-d), confirms the first order kinetics for the decomposition process. According to the kinetic data obtained from the TG curves, all the complexes have negative entropy, which indicate that the complexes are formed spontaneously. The negative value of entropy indicates a more ordered activated state that may be possible through the chemisorptions of oxygen and other decomposition products. The negative values of the entropies of activation are compensated by the values of the enthalpies of activation, leading to almost the same values for the free energy of activation [17].

Table 4: Selected bond length(Å) and angle(^{0})for complexes II and III

Complexes	**Bond length (Å)**		**Bond Angles(°)**	
Complex II	16-10	1.8558	1-16-10	91.8809
	16-1	1.8059	17-16-19	88.6387
	16-19	1.8339	17-16-1	170.418
	16-17	1.8585	19-16-10	167.155
	17-18	1.3165	17-16-10	81.7281
	19-20	1.3832	19-16-1	98.6763
	20-21	1.411	16-19-31	102.686
	18-21	1.4628	20-19-31	119.248
	19-31	1.4165	16-17-18	97.3437
	2-9	1.8059	16-1-9	104.432
	1-2	1.3882	16-10-4	103.043
	10-4	1.3211	16-1-2	122.544
	4-3	1.4735	14-11-12	113.974
	18-22	1.4198	28-26-27	110.337
	22-23	1.3808	9-1-2	119.174
	21-25	1.4013		
	4-5	1.4163		
	3-8	1.42		
Complex III	16-10	1.9191	1-16-10	98.2308
	16-1	1.9645	17-16-19	95.8283
	16-19	1.9177	17-16-1	100.396
	16-17	1.8772	19-16-10	99.5898
	17-18	1.3124	17-16-10	149.096
	19-20	1.3544	19-16-1	112.393
	20-21	1.4121	16-19-31	127.672
	18-21	1.444	20-19-31	107.656
	19-31	1.5305	16-17-18	122.303
	2-9	1.4616	16-1-9	147.288
	1-2	1.3052	16-10-4	79.9504
	10-4	1.3351	16-1-2	96.9305
	4-3	1.4575	14-11-12	113.102
	18-22	1.4207	28-26-27	108.002
	22-23	1.3822	9-1-2	115.748
	21-25	1.4118		
	4-5	1.4414		
	3-8	1.3989		

3.3 Molecular modeling studies

Molecular mechanics attempts to reproduce molecular geometries, energies and other features by adjusting bond length, bond angles and torsion angles to equilibrium values that are dependent on the hybridization of an atom and its bonding scheme(Table 4: Bond length and bond angles of complex II and complex III). In order to obtain estimates of structural details of these complexes, we have optimized the molecular structure of complexes. Energy minimization was repeated several times to find the global minimum. The energy minimization value for square planar and without restricting the structure for the Ni(II) and Cu(II) complexes are almost same i.e, 6341kcal/mol with gradient 0.930 and 6210kcal/mol with gradient 0.987 respectively. This supports square planar geometry of the metal complexes [29]. The optimized molecular structure of the Ni(II) and Cu(II) complexes are represented in Figure 6a-b. The energy minimization values for copper complex has minimum than nickel complex than cobalt complex than zinc complex which has maximum energy. It indicates copper complex has maximum stability than other metal complexes.

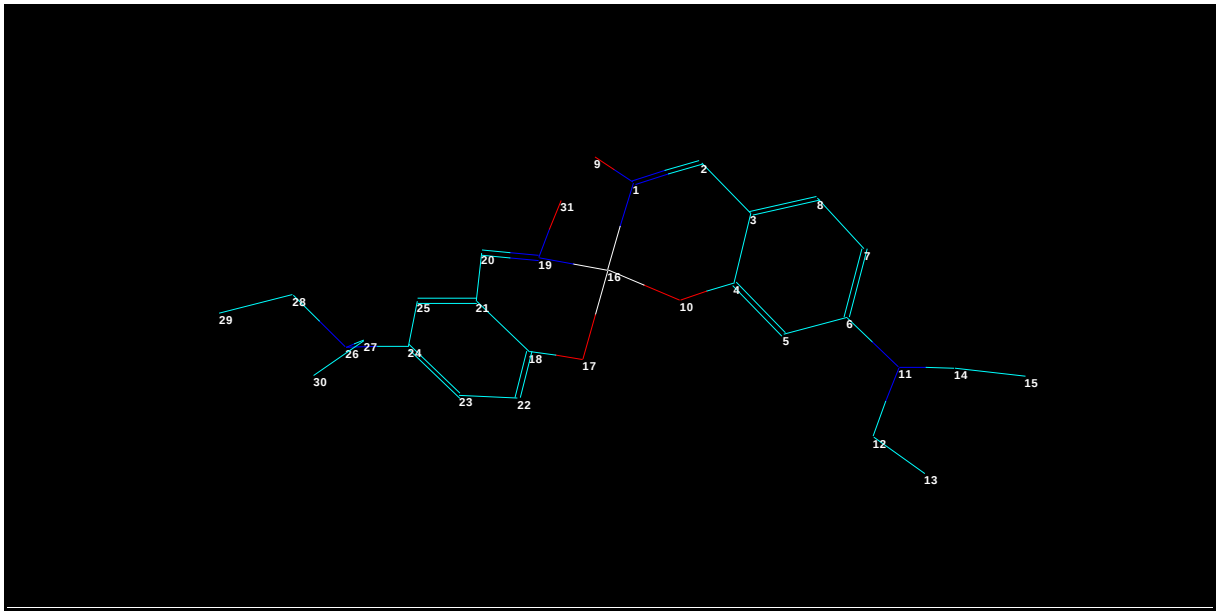

Fig. 6a: Molecular modeling of the complexes II

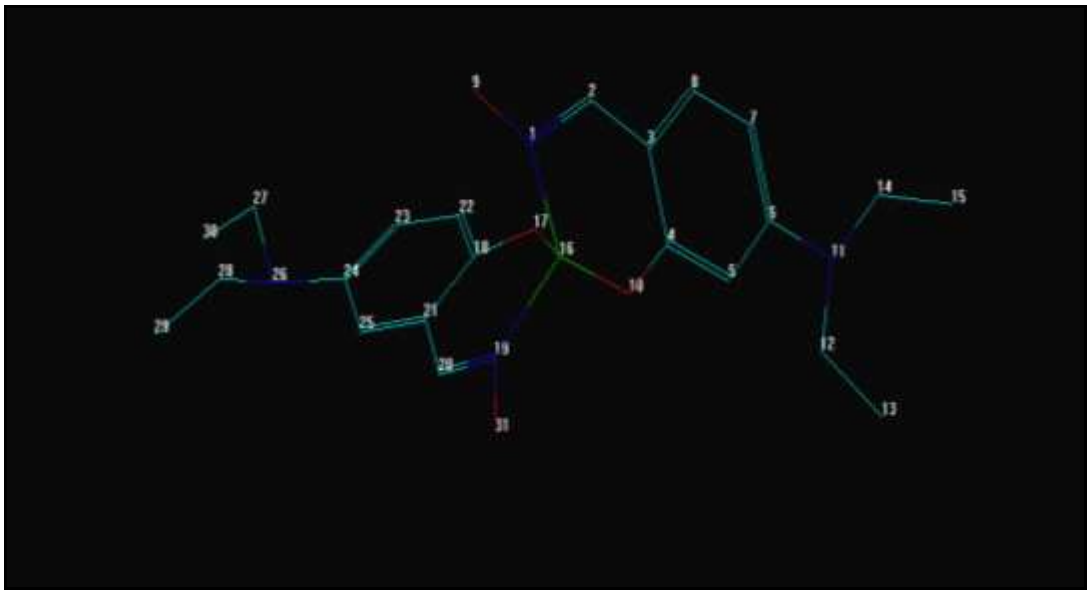

Fig 6b: Molecular modeling of complex III

3.4. Biological studies

The free ligand and its respective metal complexes were screened against *A. alternate*, *A. flavus*, *A. nidulence* and *A. niger* fungi and *Streproproteus*, *Staph*, *Staphylococcus* and *E. coli* bacteria to assess their potential antimicrobial agents. The results are quite promising. It is clear from the antifungal screening data (Fig. 7a), that the metal complexes are more fungitoxic than the chelating agent itself. The complexes showed maximum activity against *A. niger* fungi. The bacterial screening results (Fig. 7b) reveal that the free ligand showed the maximum activity against *Staphylococcus* bacteria. Its metal complexes also showed the maximum activity against *Staphylococcus bacteria* except zinc complex showed the maximum activity against *Streproproteus* bacteria. In general, the activity was the least against *Staph* bacteria. The presence of nitrogen and oxygen donor groups in the synthesized compounds inhibited enzyme production because enzymes require free hydroxyl group for their activity appear to be especially susceptible to deactivation by the metal ion [19]. Complexation reduces the polarity of the metal ion from partial sharing of its positive charge with the donor groups; π- electron delocalization in this chelating ring also increases the lipophilic nature of the metal atom, favoring permeation through the lipid layer of the membrane. The enhanced activity of the metal complexes may be ascribed to the increased lipophilic nature of these complexes arising due to chelation [19]. It was also noted that the toxicity of the metal chelates increases on increasing the metal ion concentration. It is probably due to faster diffusion of the chelates as a whole through the cell membrane or due to the chelation theory. The bounded metal may block enzymatic activity of the cell or else it may catalyze toxic reactions among cellular constituents.

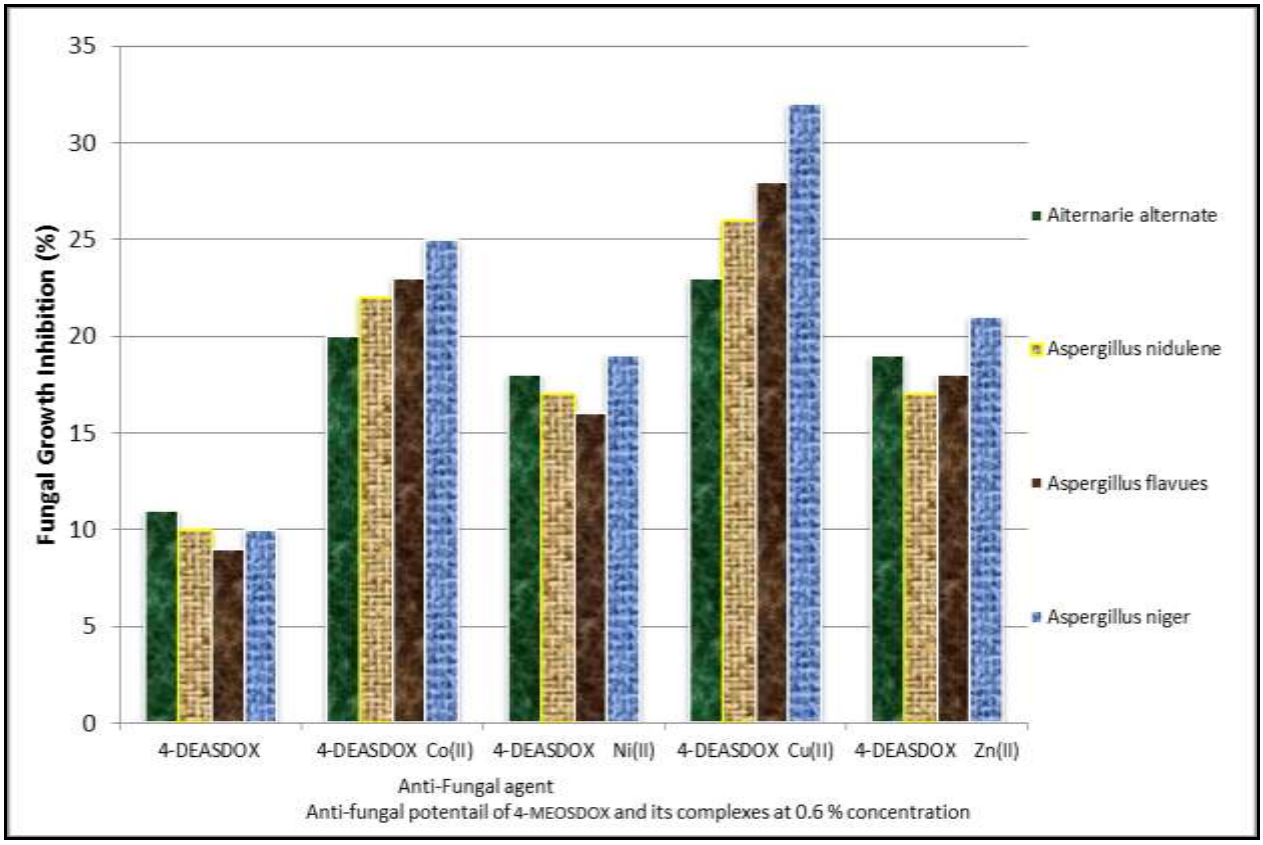

Fig.7a : Antifungal potential of ligand and its metal complexes at 0.6% concentration

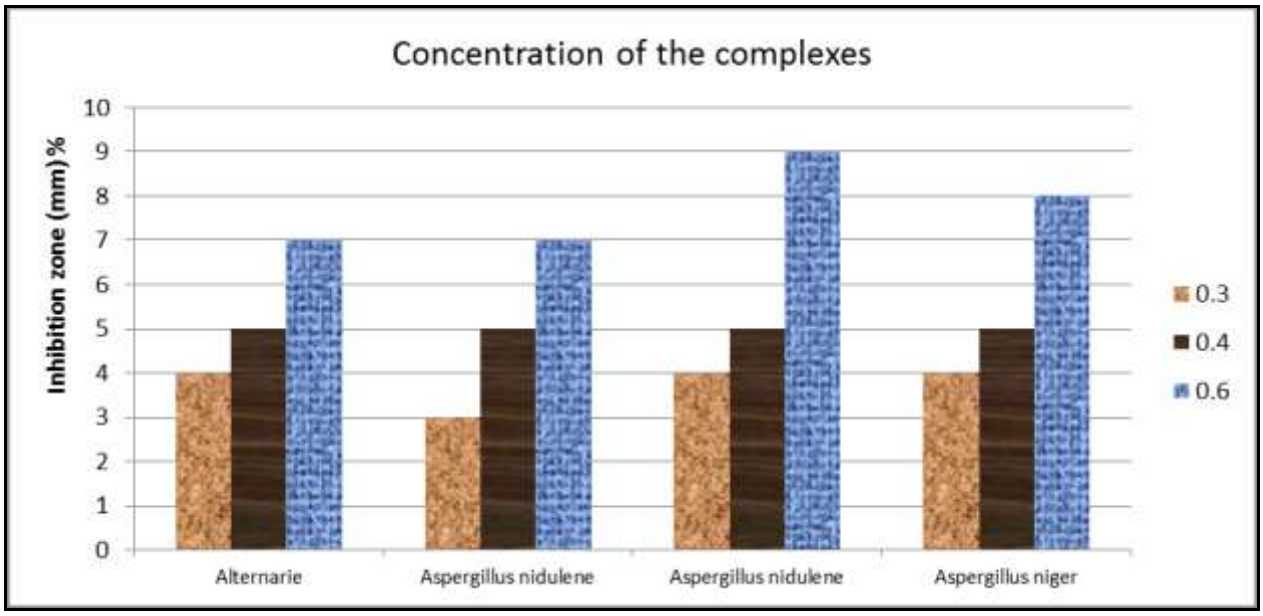

Fig.7b: Effect of concentration of complex III and its antifungal potential

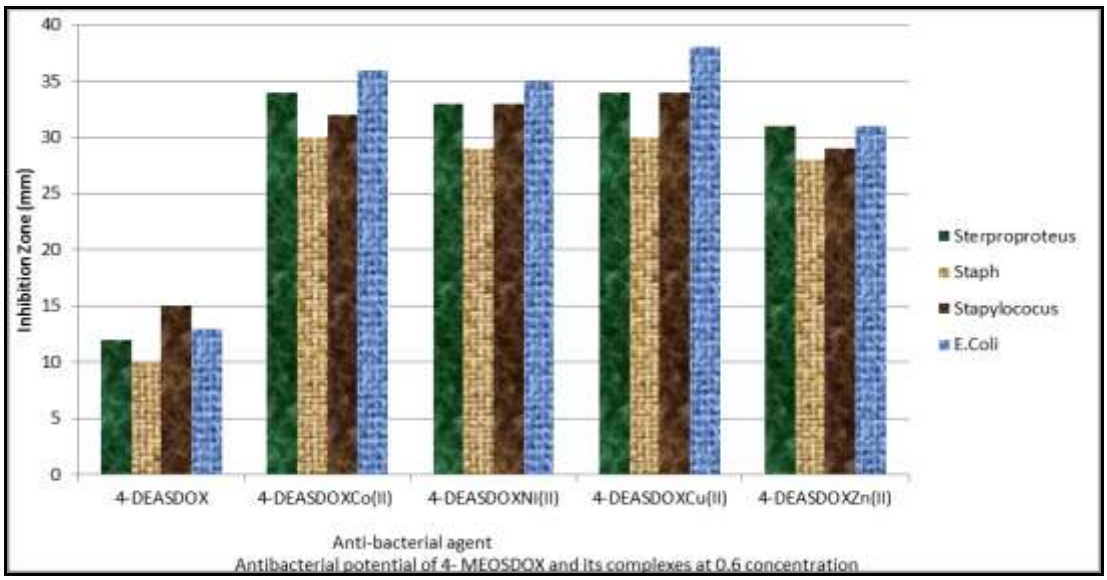

Fig.7c: Anti-bactrial potential ligand and its complexes at 0.6%

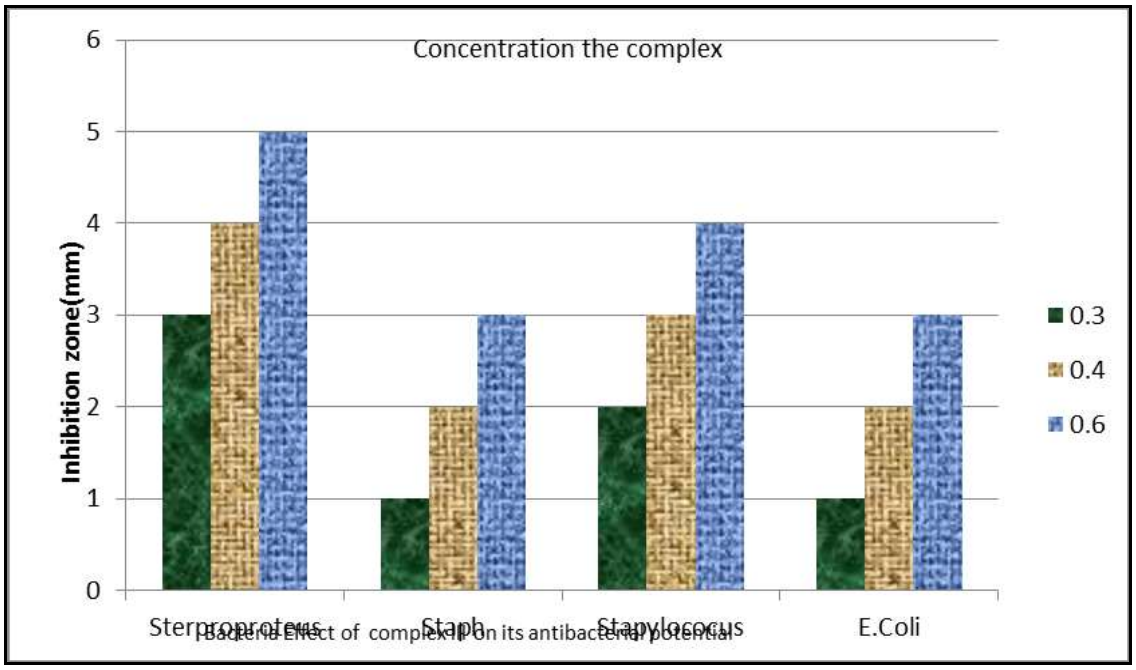

Fig.7d: Effect of concentration of complex III & its anti-bacterial potential

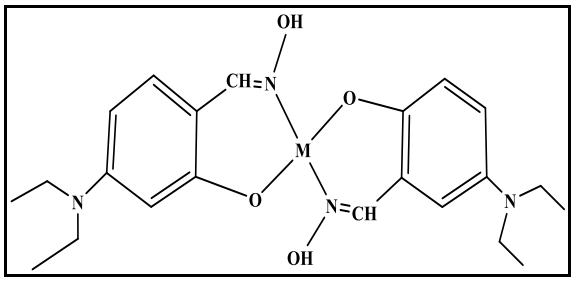

Fig.8: Proposed structure of metal- 4-DEASOX complexes, Where M= Cu(II),Co(II),Ni(II) and Zn(II) .

4. Conclusion

With the help of various physico-chemical techniques, geometries of the newly synthesized compounds have been proposed (Figure 8). The ligand acts as a bidentate ligand involved coordination with metal ions through the phenolic oxygen and the oxime nitrogen forming square planar complexes. Kinetics of thermal decomposition was computed from the thermal data using Coats and Redfern method, which confirm first order kinetics. The Cu(II) complex was found to be most active against the growth of bacteria and pathogenic fungi.

Acknowledgements

The author (B K Singh) thankfully acknowledge to University Grants Commission(UGC), New Delhi, India for financial support.

References

1. (a) Durmus M. Dincer F. Ahsen V. Dyes and Pigments 2008,77, 402-407.(b)Abele E. Lukevics E. Org. Prep. Proceed Int. 2000,32,235-264.(c) Chakravorty A. Coord. Chem. Rev. 1974,13,1-46.(d) Ramesh V. Umasundari P. Das K. K. Spectrochimica Acta Part A 1998,54, 285–297.
2. (a) Martinez J. Aiello I. Bellusci A.Crispini A. Ghedini M.Inorganic Chim Acta 2008, 361, 2677-2682.(b)Gumus G. Ahsen V.*Mol*. Cryst Liq Cryst. 2000, 348, 167-178.(c)Ohta K, Hasebe H. Moriya M. Fujimoto T.Yamamoto I. Mol Cryst Liq Cryst 1991, 208, 43-54.
3. Jayaraju D.Kondapi A. K. Current Science 2001,81(7), 787-792.
4. Březina F. Tillmannová H. And Šindelář Z.Chem. Papers ,1986, 40(6), 727—733.

5. Rajabi L. Courreges C.Montoya J. Aguilera R. J.Primm T. P. Lett. Appl. Microbiol. 2005, 40, 212-215.
6. Hyperchem Release 7.51 Professional Version for Windows, Molecular Modeling System, Hyperchem Inc. Canada, 2005.
7. Saxena C.Sharma D. K. Singh R. V. Phosphorous Sulfur Silicon 1993, 85(1-4), 9-1
8. Omar M. M. Mohamed G. G. Spectrochim. Acta A,2005, 61, 929.
9. Georgieva I.Tredafilova N. Bauer G. Spectrochim. Acta A 2006, 63, 403
10. Nakamoto K. Infrared and Raman Spectra of Inorganic and Coordination Compounds, Wiley, New York, 1978.
11. Silverstein R. M. Bassler O. G.Morrill T. C. Spectrophotometic Identification of Organic Compounds, Wiley, New York, 1974.
12. Nakamoto K, McCarthy S.J, Spectroscopy & Structure of Metal Chelate Compounds, John Wiley & Sons, USA, 1968.
13. Lever A.B P, Inorganic Electronic Spectroscopy, Elsevier, Amsterdam, 1968.
14. Figgis B N, Introduction to Ligand Fields, 1st ed., 1966, p. 263.
15. (a) Sanmartin J. Novio F. Garcia- Deibe A. M.Fondo M.Ocampo N. Bermejo M. R. Polyhedron ,2006, 25, 1714-1722. (b) Singh B. K. Prakash A. Adhikari D. Spectrochim. Acta A 2009, 74, 657-664.(c) Singh B. K. Rajour H. K. Prakash A. Spectrochim. Acta A,2012, 94, 143-151.(d) Beloso I. Castro J. Garcia-Vazquez J. Perez-Lourido A. P. Romero J. Sousa A, Polyhedron,2003, 22, 1099-1111.
16. (a) Yoshida N. Ichikawa K. Shiro M. J. Chem. Soc.Parkin *Trans*. 2000, 2, 17-26. (b) Yoshida N. Oshio H.Ito T.J. Chem. Soc. Perkin Trans.1999, 2, 975-984.(c) Singh B.K. Rajour H.K. Chauhan R. Goyal S. Chemical Sci. Transections 2015, 4(3), 806-818.
17. a) Singh B K , Sharma R.K, Garg B S, J. Thermal Anal. Cal.2006, 84, 593. (b) Prakash A, Singh B. K., Bhojak N, Adhikari D, Spectrochim Acta A 2010, 76, 356-362.
18. Coats W, Redfern J, P, Nature, 1964,201 68-69.
19. (a) Ahamad T. Nishat N. Parveen S. J. Coord. Chem. 2008, 61, 1963-1972 (b) Singh B. K,.Rajour H. K, Chandra J. J. Applied Chemical Sci. International, 2016, 6(1), 45-57.(c) Singh B.K, Mishra P, .Prakash A,,Bhojak N, Arabian J .Chem.2017, 10,S472-S483.

*****